Influence of Water in the UV-Induced Chemistry of Methanol in the Solid Phase

L. Krim,*,† J. Lasne,‡ C. Laffon,§ and Ph. Parent§

Laboratoire de Dynamique, Interactions et Réactivité, Université Pierre et Marie Curie-Paris 6, CNRS, UMR 7075, Case courrier 49, Bât F 74, 4 place Jussieu, 75252 Paris Cedex 05, France, and UPMC Univ Paris 06 and CNRS, UMR 7614, Laboratoire de Chimie Physique, Matière et Rayonnement, 11 rue Pierre et Marie Curie, 75231 Paris Cedex 05, France

Received: May 15, 2009; Revised Manuscript Received: June 24, 2009

UV-irradiated methanol (CH_3OH) in water ice at 3 K has been investigated with infrared spectroscopy and compared with pure methanol. The main byproducts detected are formaldehyde (H_2CO), carbon monoxide (CO), carbon dioxide (CO_2), methane (CH_4), and ethylene glycol ($C_2H_4(OH)_2$). The production of H_2CO, CO_2, and CO is enhanced in water ice, resulting from cross reactions between the byproducts of methanol with those of water (OH and H_2O_2).

I. Introduction

Methanol is one of the constituents of the icy mantle of the interstellar grains and of a number of inner or outer solar system corpses, where it is trapped in water ice and processed by space radiation. The photolysis of methanol then occurs in the presence of water, giving rise to simple or more complex byproducts that must be identified for a comprehensive understanding of the role of methanol in astrochemistry. In the laboratory, the photochemistry of condensed methanol has been repeatedly examined in the past decades. Pure methanol ices have been irradiated with UV,[1−3] ions,[4] and He^+ ions, and UV,[5] electrons[6] and protons.[7] These studies have shown that methanol decomposition leads to CO, CO_2, CH_4, H_2CO,[1,2,4−7] HCO,[1,2,6,7] H_2,[1,2] CH_2OH,[6] methyl formate (H_3COHCO),[2,6] and ethylene glycol ($C_2H_4(OH)_2$).[6] So far, the irradiation of methanol in water has been only sparsely investigated. Methanol and water mixtures have been studied after exposure to UV,[3,8] He^+ ions,[9,10] and protons.[7,11] These works have shown that, qualitatively, the presence of water makes no difference in the nature of the generated species; the byproducts are essentially the same as those in pure methanol: CO, CO_2, CH_4,[7−11] H_2CO,[7,8,10] $HCOO^-$,[11] HCO,[7,8] and ethylene glycol.[11] Quantitative analysis of their production has also been reported, although not in a detailed manner.[7,9,10] It has been shown, in particular, that the CO/CO_2 ratio decreases as the water content increases, possibly caused by an oxidation of CO into CO_2 by the water byproducts. Accounting for the importance of the methanol−water system in astrochemistry, the understanding of the influence of water in the irradiation-induced chemistry of methanol is important to deepen. For this purpose, we have undertaken the infrared study of the UV irradiation at 3 K of pure methanol and methanol in ice at various water concentrations. We have first identified the byproducts formed after irradiation of pure and diluted methanol. From the column densities derived from the infrared spectra, we have built for H_2CO, CO_2, and CO a quantity allowing the comparison of their efficiency of formation in the various environments. This clearly evidences the strong role of water in the formation of some of the major species and allows us to discuss a possible reaction scheme involving the fragments of methanol and those of water.

II. Experimental Section

The CH_3OH/H_2O (and CH_3OH/Ne) films were prepared by co-condensation of CH_3OH and H_2O (or Ne) on a cryogenic metal mirror (1 cm^2) maintained at 3 K by a pulsed tube closed-cycle cryogenerator (Cryomech PT405). The setup was evacuated at 7×10^{-8} mbar before refrigeration of the sample holder. Neon gas was obtained from Air Liquide with purity of 99.9995%. Natural water and methanol (Prolabo RP grade) were degassed under vacuum. The purity of the samples was confirmed spectroscopically. The deposition rates were 10 μmol/min. Accounting for the dosing time, this gives a film thickness of about 1 μm, but the thickness was not directly measured. The film compositions were deduced from the partial pressures of each of their components in the gas phase, assuming a sticking coefficient of unity for methanol, water, and neon at 3 K. The IR spectra were recorded in the transmission-reflection mode between 4500 and 500 cm^{-1} (resolution 1 cm^{-1}) using a Bruker 120 FTIR spectrometer equipped with a KBr/Ge beamsplitter and a liquid-N_2-cooled narrow band HgCdTe photoconductor. Bare mirror backgrounds recorded from 4500 to 500 cm^{-1} prior to the sample deposition were used as references in processing the sample spectra. The absorption spectra in the mid-infrared were collected on samples through a KBr window mounted on a rotatable flange separating the interferometer vacuum (10^{-3} mbar) from that of the cryostatic cell (10^{-7} mbar). The spectra were subsequently corrected from a baseline to compensate for infrared light scattering and interference patterns. All spectra were recorded at 3K to stop or limit the diffusion of the photoproducts. For each methanol concentration, the spectra were directly recorded after deposition and after exposure to photons at chosen irradiation times. The UV source was a krypton lamp (Resonance Ltd.) interfaced with the vacuum chamber through a LiF window transmitting $\lambda >$ 104 nm. Its spectrum is composed of two intense peaks at 116.5 (10.64 eV) and 123.6 nm (10.04 eV), accounting for 60% of the total intensity, and a broad continuum in the 130−170 nm (7.3−9.5 eV) range, centered at 148 nm (8.38 eV), accounting

* Corresponding author. E-mail: krim@ccr.jussieu.fr.
† Laboratoire de Dynamique, Interactions et Réactivité, Université Pierre et Marie Curie-Paris 6.
‡ UPMC Univ Paris 06, UMR 7614, Laboratoire de Chimie Physique, Matière et Rayonnement.
§ CNRS, UMR 7614, Laboratoire de Chimie Physique, Matière et Rayonnement.

10.1021/jp904534a CCC: $40.75
Published on Web 07/10/2009

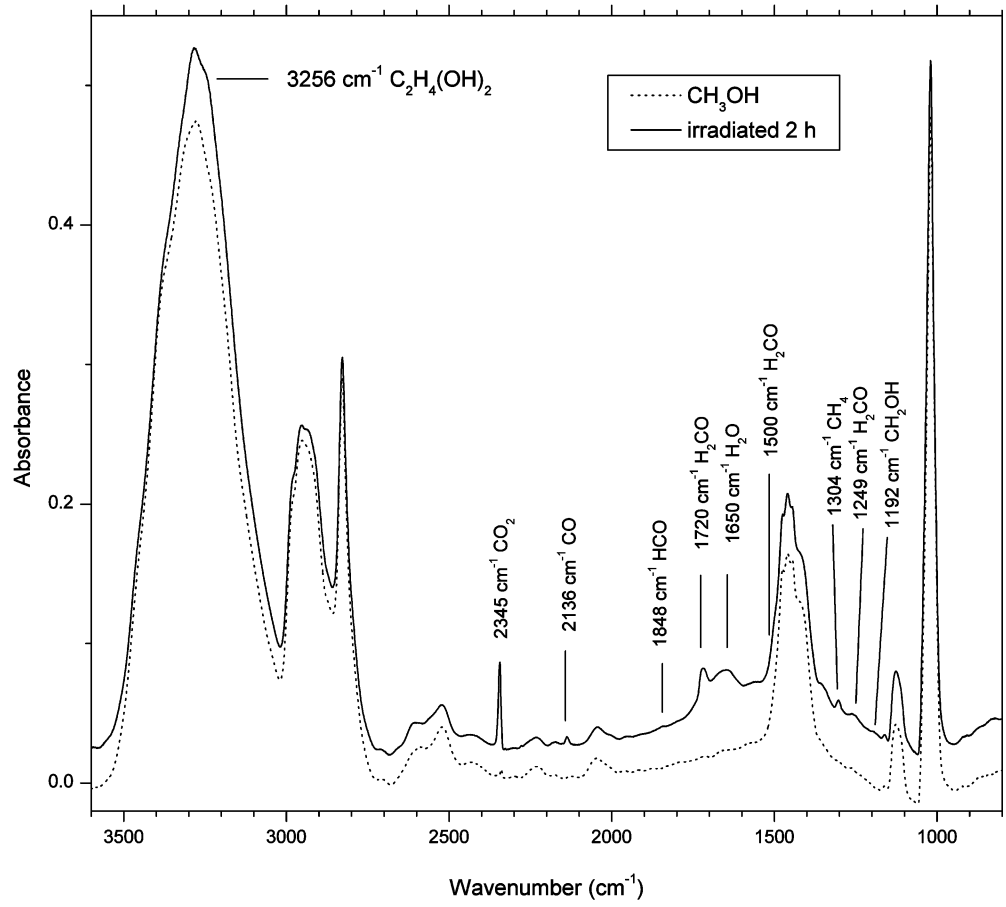

Figure 1. Infrared spectrum of pure methanol at 3K before (dotted line) and after 2 h of irradiation (31.6 eV·molecule^{-1}) (solid line) with the band assignments of the byproducts.

for 40% of the total intensity. The total flux at the sample was 1.7×10^{14} photons·s^{-1}, as deduced from the sample−source distance and from the flux provided by the manufacturer of the source. Because the source is not monochromatic, the irradiation dose per molecule cannot be calculated. For sake of comparison with other studies, we propose an estimation of the dose by calculating the mean energy of the UV beam and doing a linear combination formed by the spectral weight of the main emission lines at 10.04 and 10.64 eV (60%) and that of the underlying continuum from 7.3 to 9.5 eV (40%; this continuum is approximated by a broad Gaussian line centered at the mean energy of 8.4 eV). This gives a mean energy per incident photon on the sample of 9.52 eV. The energy received by each molecule of the sample is 4.4×10^{-3} eV·s^{-1}·molecule^{-1}. The films were irradiated for 2 h, corresponding to a total estimated exposition of 31.6 eV·molecule^{-1}.

The samples studied are pure methanol, pure water, mixtures of methanol in water (H_2O/CH_3OH) with 1:1 and 10:1 molar compositions, and a mixture of methanol in neon (Ne/CH_3OH) with 1:1 molar composition.

III. Results

Figure 1 shows the IR spectrum of solid methanol recorded between 500 and 4500 cm^{-1} before and after 2 h of UV irradiation at 3 K. Before irradiation, four spectral regions with very intense IR absorption bands are observed: (1) the CO stretching and CH_3 rocking modes around 1000 cm^{-1}; (2) the symmetric and asymmetric CH_3 bending modes and also the OH bending mode around 1500 cm^{-1}; (3) the symmetric and asymmetric CH stretching modes near 3000 cm^{-1}; and (4) the OH stretching mode around 3300 cm^{-1}. Several harmonic and combination bands are also detected between 2000 and 2700 cm^{-1}. The peak positions of the main features are reported in Table 1.

TABLE 1: Peak Positions of the Main Spectroscopic Features of Condensed Methanol

vibration mode	wavenumber (cm^{-1})
O−H stretch	3280
CH_3 stretch (asym)	2954
CH_3 stretch (sym)	2828
CH_3 rock + OH bend	2521
CH_3 rock (overtone)	2232
CO stretch (overtone)	2049
CH_3 bend (asym)	1477
CH_3 bend (sym)	1445
OH bend	1422
CH_3 rock	1126
CO stretch	1020

After the irradiation, several products are observed through their characteristic fingerprints:[6] formaldehyde H_2CO at 1720, 1500, and 1249 cm^{-1}; methane CH_4 at 1304 cm^{-1}; the formyl radical HCO at 1848 cm^{-1}; ethylene glycol (EG) $C_2H_4(OH)_2$ at 3256 cm^{-1}; carbon monoxide (CO) at 2136 cm^{-1}; carbon dioxide (CO_2) at 2345 cm^{-1}; hydroxymethyl radical (CH_2OH) at 1192 cm^{-1}; and water H_2O at 1650 cm^{-1}. Methyl formate H_3COHCO (1718 cm^{-1})[2] is not detected. The methoxy radical (CH_3O) cannot be directly observed because most of its absorption bands overlap those of methanol.[6]

These observations are consistent with the works published to date, except for water. Water has been reported only by

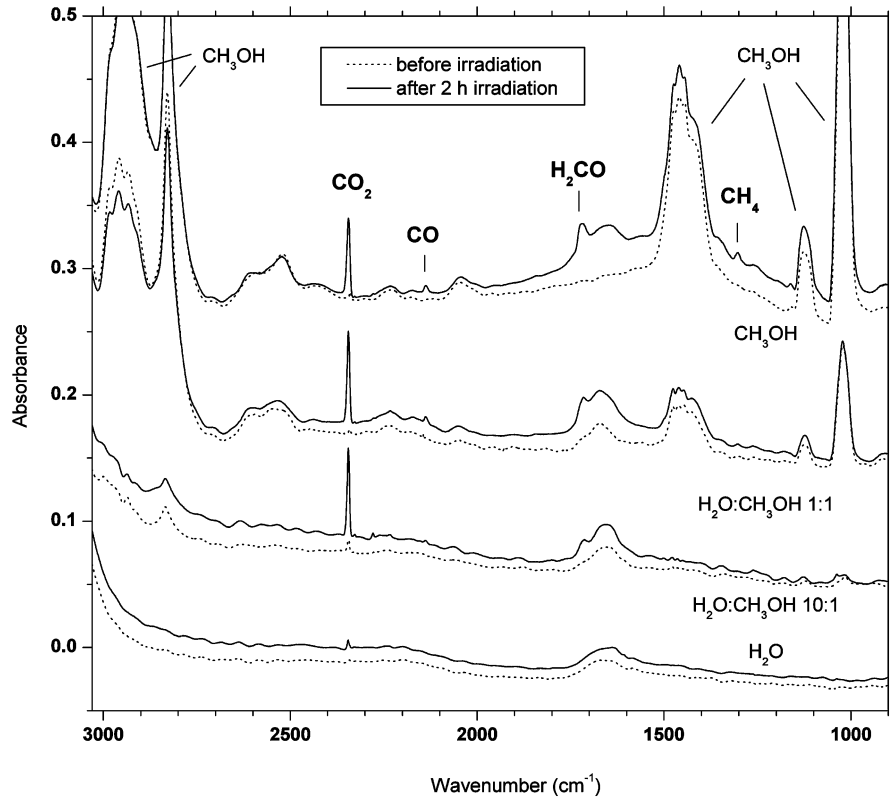

Figure 2. Infrared spectra of CH_3OH in H_2O ice at 3K before (dotted line) and after 2 h of irradiation (solid line) for pure CH_3OH (0:1), H_2O/CH_3OH (1:1 and 10:1), and pure H_2O (1:0).

Baratta et al.[9] and, later, in the same group, by Palumbo et al.,[4] who assume that this byproduct results from the methanol decomposition. Bennett et al.[6] and Schutte et al.[1] have observed the same species as those in the works of Baratta and Palumbo, except water. This indicates that H_2O is probably not generated by the irradiation of methanol. Rather, we suggest that its presence is caused by the contamination of the sample surface with time. Because the low temperature prevents water from migrating into the bulk, we assume that its contribution to the photochemistry of methanol (pure or in water) is restrained to the surface layer and can be neglected in the context of this work.

Figure 2 presents the spectra before and after 2 h of irradiation at 3 K of the H_2O/CH_3OH ices with 0:1 (pure methanol), 1:1, 10:1, and 1:0 (pure water) composition. At 1:1 and 10:1 dilutions, we clearly observe the characteristic features of CO_2, CO, and H_2CO, as in pure methanol. Methane and ethylene glycol are detected in the 1:1 spectrum, but in the 10:1 spectrum, their intensities are lost in the background. The intensity of the CO stretching mode of CO_2 at 2345 cm^{-1} remains almost constant over all water concentrations. This indicates that the CO_2 formation is enhanced in the presence of water. We also note that the intensity of CO_2 remains weak in pure water ice (6×10^{-3}), showing that contamination by CO_2 is negligible.

To evidence the role of water in the generation of CO_2 further, we compare in Figure 3 the irradiation of 50% of methanol in water and in neon, which cannot react with the methanol byproducts. The intensity of the CO stretching mode of CO_2 at 2345 cm^{-1} is 7 times lower in neon than in water. This, again, shows the enhancement in the production of CO_2 in the presence of water.

Besides the case of CO_2, it is useful to estimate how the yield of the other byproducts is sensitive to the presence of water. For this, we have defined Y(X), the yield of species X per

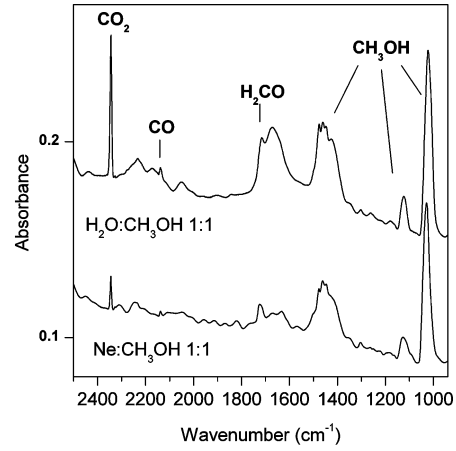

Figure 3. Infrared spectra after 2 h of irradiation at 3K for the H_2O/CH_3OH 1:1 and Ne/CH_3OH 1:1 mixtures.

methanol destroyed. This is calculated by the ratio $Y(X) = [X]/\Delta[CH_3OH]$, where [X] is the column density of the species X, and the amount of methanol destroyed, $\Delta[CH_3OH]$, is obtained by the difference between the column density of CH_3OH before and after irradiation (as derived from the band at 1020 cm^{-1}). Note that the amount of irradiated methanol over the amount of methanol probed by the infrared beam may vary from one sample to another, depending on the film thickness and its composition. The difference $\Delta[CH_3OH]$ naturally corrects the quantity Y(X) from these possible variations and allows a direct comparison of the efficiency in the generation of X in the different samples. Y(X) indicates how efficient the conversion of CH_3OH into the X species is, independently of the methanol concentration into the sample. The higher the Y value is, the highest this efficiency is.

The Y(X) values were determined for the species with a well-separated IR band and owning measurable intensities at low

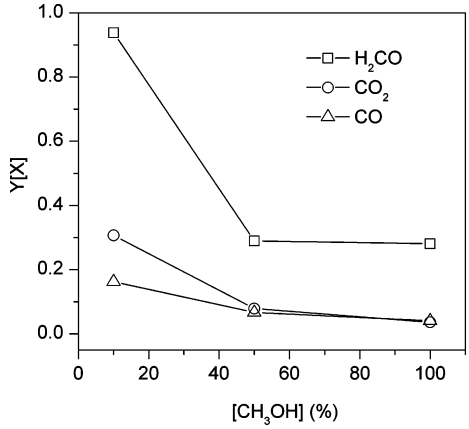

Figure 4. Yield of CO_2, CO, and H_2CO per methanol destroyed ($Y(CO_2)$, $Y(CO)$, and $Y(H_2CO)$) after 2 h of irradiation as a function of methanol concentration in the water matrix. Lines are to guide the eyes.

methanol concentrations, such as CO_2, CO, and H_2CO. The column densities, [X], are obtained by multiplying the integrated areas of the absorption bands by the associated band strengths, A: (1) the CO stretching mode of CH_3OH at 1020 cm^{-1}, $A = 1.3 \times 10^{-17}$ cm·molecule^{-1};[4] (2) the CO stretching mode of CO_2 at 2345 cm^{-1}, $A = 2.1 \times 10^{-16}$ cm·molecule^{-1};[12] (3) the stretching mode of CO at 2136 cm^{-1}, $A = 1.7 \times 10^{-17}$ cm·molecule^{-1};[12] and (4) the CO stretching mode of H_2CO at 1720 cm^{-1}, $A = 1.8 \times 10^{-17}$ cm·molecule^{-1}.[6] Mixing of this band with the CO stretching of acetone ($(CH_3)_2CO$) has been sometimes evoked[9] and then ruled out.[11] We do not see any other characteristic features of acetone (at 1444, 1232, and 1090 cm^{-1})[9] indicating that its concentration is negligible. Therefore, the band at 1720 cm^{-1} is assigned solely to H_2CO.

We assume that the variations in the band intensities are mainly due to variations in the concentration of the species and not to changes in the coupling between the considered species and the water lattice as the water concentration varies. This has been well established at least for CO and CO_2, where only minor changes in A are observed with the dilution in water.[13] This allows us to compare the Y values relatively from one concentration to another safely. However, because of the spread on the published band strength values, the absolute values of Y must be taken with some caution.

Figure 4 shows $Y(H_2CO)$, $Y(CO_2)$, and $Y(CO)$ after 2 h of UV irradiation as a function of the methanol concentration in water. The Y values all increase with the methanol dilution, showing that the production of CO, CO_2, and H_2CO becomes more efficient as the methanol content decreases. This is especially marked for CO_2 at low methanol concentrations, where its yield in the 10:1 sample is 7.5 times higher than that in pure methanol. This is also true for H_2CO and CO, whose yields in the 10:1 sample are 3.3 and 4 times higher than those in pure methanol, respectively. This is the main outcome of this study: the formation of H_2CO, CO_2, and CO is strongly favored when methanol is diluted in water.

As other authors did,[7,9,10] we have calculated the CO/CO_2 ratio from the column densities of these two molecules. After 2 h of irradiation (31.6 eV·molecule^{-1}), we found $CO/CO_2 = 1.1$ in pure methanol, $CO/CO_2 = 0.84$ in the 1:1 sample, and $CO/CO_2 = 0.5$ in the 10:1 sample. This ratio decreases as the water concentration increases: there is more CO than CO_2 in pure methanol and more CO_2 than CO when methanol is diluted in water. This confirms the works of Moore et al.[7] and Strazzulla and Baratta et al.[9,10] These ratios are also in excellent agreement with those reported in refs 9 and10 for similar compositions and doses.

IV. Discussion

We now discuss some possible formation mechanisms leading to the observed molecules in pure methanol and when methanol is diluted in water on the basis of the published works carried out in the gas phase or in the condensed phase. We start the discussion with the photolysis routes in pure methanol. We then discuss the possible mixing of these routes with those of water and how it explains the observation reported in Figure 4.

Pure Methanol. In the gas phase below 180 nm, four primary photolysis processes have to be considered[14]

$$CH_3OH + h\nu \rightarrow CH_3O + H \quad (1)$$

$$\rightarrow CH_2OH + H \quad (2)$$

$$\rightarrow H_2CO + H_2 \quad (3)$$

$$\rightarrow CH_3 + OH \quad (4)$$

Reactions 1 and 2 dominate.[6]

A further decomposition reaction has been evoked in the condensed phase irradiated with 5 keV electrons[6]

$$CH_3OH + h\nu \rightarrow CH_4 + O \quad (5)$$

Methane is also produced by recombination of CH_3 (reaction 4) with H emitted by the methanol photolysis (reactions 1 and 2)[15]

$$CH_3 + H \rightarrow CH_4 \quad (6)$$

A possible recombination of methanol with excited H* is sometimes mentioned.[6]

$$CH_3OH + H^* \rightarrow CH_2OH + H_2 \quad (7)$$

$$CH_3OH + H^* \rightarrow CH_3O + H_2 \quad (8)$$

In the condensed phase, CH_2OH produced by reactions 2 and 7 recombines into ethylene glycol[16,17]

$$CH_2OH + CH_2OH \rightarrow C_2H_4(OH)_2 \quad (9)$$

At 3 K, the diffusion of the hydroxymethyl fragment (CH_2OH) is reduced, and reaction 9 most likely occurs between two adjacent CH_2OH fragments. Therefore, the production of ethylene glycol should drop with the CH_2OH concentration and hence with that of methanol.

Dehydrogenation of the methoxy radical CH_3O produced by reactions 1 and 8 leads to formaldehyde (H_2CO)[6]

$$CH_3O + h\nu \rightarrow H_2CO + H \quad (10)$$

Reaction 10 has a barrier of 1.52 eV (817 nm),[18] which is easily exceeded by the photons of 116 nm used in the present work.

Formaldehyde produced by reactions 3 and 10 is transformed into HCO and CO by reactions 11 and 12, in which the latter dominates[6]

$$H_2CO + h\nu \rightarrow HCO + H \quad (11)$$

$$H_2CO + h\nu \rightarrow CO + H_2 \quad (12)$$

The gas-phase reactions 11 and 12 start at wavelength <340 nm.[19]

A further dehydrogenation reaction is the decomposition of HCO with H[20]

$$HCO + H \rightarrow CO + H_2 \quad (13)$$

Photolysis of HCO in H + CO is also possible at wavelength <260 nm.[21]

$$HCO + h\nu \rightarrow CO + H \quad (14)$$

CO is further oxidized by recombination with an excited CO molecule (the Boudouard reaction)[22]

$$CO^* + CO \rightarrow CO_2 + C \quad (15)$$

The diffusion of CO is unlikely at 3 K, and reaction 15 can occur only between two adjacent CO molecules.

The set of reactions 1−15 shows that the expected byproducts from the methanol decomposition are CH_3O, CH_2OH, $C_2H_4(OH)_2$, H_2CO, HCO, CH_4, CO, CO_2, H, and H_2. This is very consistent with the detection of CH_2OH, $C_2H_4(OH)_2$, H_2CO, HCO, CH_4, CO, and CO_2 in our experiments. (We recall here that CH_3O is not detectable because it may overlap with the methanol bands).

Methanol in Water. The photodecomposition of H_2O starts at $\lambda < 190$ nm.[23] It produces mainly OH and H[24,25]

$$H_2O + h\nu \rightarrow OH + H \quad (16)$$

The OH radicals can recombine to from H_2O_2[24,25]

$$OH + OH \rightarrow H_2O_2 \quad (17)$$

In pure water ice, OH and H_2O_2 are the most concentrated oxygen-bearing photoproducts and have the same abundance.[24] On the contrary, O_2, HO_2, and O are minor byproducts, and their reactions can be neglected.[24] The OH, H, and H_2O_2 radicals can combine with CH_3OH and its fragments

First, methanol can be attacked by OH to produce CH_2OH and CH_3O[17,26,27]

$$CH_3OH + OH \rightarrow CH_2OH + H_2O \quad (18)$$

$$\rightarrow CH_3O + H_2O \quad (19)$$

In the gas phase, reaction 18 is six times more efficient than reaction 19, and the formation of CH_2OH dominates.[28] CH_2OH is not expected to react with OH. The only significant reaction of CH_2OH is with H_2O_2, which leads to H_2CO[27]

$$CH_2OH + H_2O_2 \rightarrow H_2CO + H_2O + OH \quad (20)$$

Formaldehyde produced by this reaction is then decomposed by OH in HCO[17,29]

$$H_2CO + OH \rightarrow HCO + H_2O \quad (21)$$

A further dehydrogenation reaction by OH leads to CO[28]

$$HCO + OH \rightarrow CO + H_2O \quad (22)$$

Finally, CO is oxidized in CO_2 by reaction with OH[30,31]

$$CO + OH \rightarrow CO_2 + H \quad (23)$$

Figure 5 summarizes all of these possible mechanisms.

These reactions lead to the same species as those in pure methanol because the UV photon and the oxidative radicals stemming from the water decomposition induce similar dehydrogenation reactions. For instance, the reaction of methanol with OH generates CH_2OH and CH_3O (reactions 18 and 19), as does the hydrogen abstraction from methanol by a photon (reactions 1 and 2). Similarly, H_2CO is produced by the UV dehydrogenation of CH_3O in pure methanol (reaction 10), whereas in water, it is formed by the reaction of CH_2OH with H_2O_2 (reaction 20). However, the yields of the photoreaction and those involving the water radicals are different (and strongly change with the water contents). The effect of water is to heighten the yields because new formation routes appear at the side of those present in pure methanol. For example, the reaction of CH_2OH with H_2O_2 (reaction 9) comes in addition to the photochemical reactions leading to H_2CO (3 and 10), so the production of H_2CO is increased in the presence of water. In the case of CO_2, the yield of the reaction CO + CO* decreases with the methanol dilution because the probability of finding two neighboring CO drops. In water, the production of CO_2 is enabled by the reaction CO + OH. This is well evidenced by the experiment presented in Figure 3, showing that the amount of CO_2 in neon is 7 times lower in the neon matrix than in water. In neon, the CO_2 concentration is built only on the CO + CO* reaction, whereas in water, the CO + OH reaction also takes place.

In water, CO is generated by the dehydrogenation of H_2CO by OH (reactions 21 and 22). The growth of Y(CO) is less marked than that for CO_2 and H_2CO (Figure 4). It is because CO can be further converted into CO_2 by reaction with OH (reaction 23), increasing the yield of CO_2 at the expense of CO. This conversion becomes more probable as the water (hence the OH) concentration increases: the amount of CO_2 can then overcome that of CO, causing the CO/CO_2 ratio to decrease with the methanol dilution.

V. Conclusions

We have evidenced the formation of H_2CO, CH_2OH, CH_4, HCO, $C_2H_4(OH)_2$, CO, and CO_2 in irradiated methanol and in methanol mixed with water ice at 3 K. The reactions of the methanol fragments with those of water (H, OH, and H_2O_2) lead to species identical to those formed in the photochemical routes of pure methanol. The formation of the byproducts is more efficient when methanol is diluted in water, especially for H_2CO and CO_2 and less markedly for CO. This allows us to substantiate the interplay between the photochemical routes of methanol with that of water. In particular, we propose that (A) in water, the production of formaldehyde is increased by the reaction of the hydroxymethyl radical CH_2OH with H_2O_2, and (B) the production of CO_2 is enhanced by the reaction of CO with OH. This reaction is a sink for CO, partially compensated

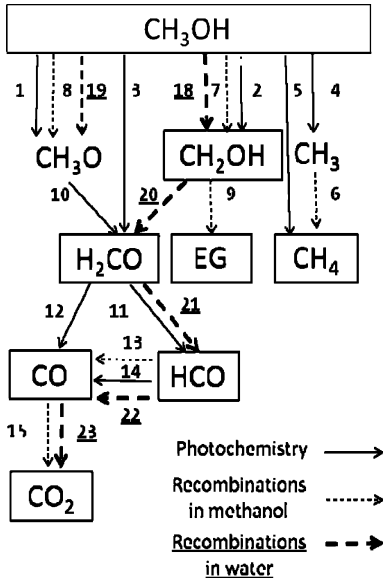

Figure 5. Schematic representation of the possible photochemical pathways that can occur in pure methanol and in methanol in water ice. Numbers refer to the reaction numbers in the text. Strict photochemical reactions are indicated in full arrows. Molecular or radical recombination reactions in pure methanol are indicated with dotted arrows; recombination reactions in water ice are indicated with bold dashed arrows, and the corresponding reaction number is underlined. Species in the boxes are those experimentally detected.

by the dehydrogenation of H_2CO into CO by the hydroxyl radical. The transformation of CO into CO_2 in the presence of water explains the decrease in the CO/CO_2 ratio when methanol is diluted into water.

References and Notes

(1) Schutte, W. A.; Gerakines, P. A. *Planet. Space. Sci.* **1995**, *43*, 1253.
(2) Gerakines, P. A.; Schutte, W. A.; Ehrenfreund, P. *Astron. Astrophys.* **1996**, *312*, 289.
(3) Cottin, H.; Moore, M. H.; Bénilan, Y. *Astrophys. J.* **2003**, *590*, 874.
(4) Palumbo, M. E.; Castorina, A. C.; Strazzulla, G. *Astron. Astrophys.* **1999**, *342*, 551.
(5) Baratta, G. A.; Leto, G.; Palumbo, M. E. *Astron. Astrophys.* **2002**, *384*, 5343.
(6) Bennett, C. J.; Chen, S.-H.; Sun, B.-J.; Chang, H. H. A.; Kaiser, R. I. *Astrophys. J.* **2007**, *660*, 1588.
(7) Moore, M. H.; Ferrante, R. F.; Nuth, J. A., III. *Planet. Space. Sci.* **1996**, *44*, 927.
(8) Allamandola, L. J.; Sanford, S. A.; Valero, G. J. *Icarus* **1988**, *76*, 225.
(9) Baratta, G. A.; Castorina, A. C.; Leto, G.; Palumbo, M. E.; Spinella, F.; Strazzulla, G. *Planet. Space. Sci.* **1994**, *42*, 759.
(10) Strazzulla, G.; Arena, M.; Baratta, G. A.; Castorina, A. C.; Celi, G.; Leto, G.; Palumbo, M. E.; Spinella, F. *Adv. Space. Res.* **1995**, *16*, 61.
(11) Hudson, R. L.; Moore, M. H. *Icarus* **2000**, *145*, 661.
(12) Sandford, S. A.; Allamandola, L. J.; Tielens, A. G. G. M.; Valero, G. J. *Astrophys. J.* **1988**, *329*, 498.
(13) Gerakines, P. A.; Schutte, W. A.; Greenberg, J. M.; van Dishoeck, E. F. *Astron. Astrophys.* **1995**, *296*, 810.
(14) Porter, R. P.; Noyes, W. A. *J. Am. Chem. Soc.* **1958**, *88*, 2310.
(15) Brouard, M.; Macpherson, M. T.; Pilling, M. J.; Tulloch, J. M.; Williamson, A. P. *Chem. Phys. Lett.* **1985**, *113*, 413.
(16) Zich, W.; Getoff, N. *Monatsh. Chem.* **1970**, *101*, 1583.
(17) Heit, G.; Neuner, A.; Saugy, P.-Y.; Braun, A. M. *J. Phys. Chem. A* **1998**, *102*, 5551.
(18) Adams, G. F.; Bartlett, R. J.; Purvis, G. D. *Chem. Phys. Lett.* **1982**, *87*, 311.
(19) Troe, J. *J. Phys. Chem. A* **2007**, *111*, 3868.
(20) Friedrichs, G.; Herbon, J. T.; Davidson, D. F.; Hanson, R. K. *Phys. Chem. Chem. Phys.* **2002**, *4*, 5778.
(21) Krasnoperov, L. N.; Chesnokov, E. N.; Stark, H.; Ravishankara, A. R. *Proc. Combust. Inst.* **2005**, *30*, 935.
(22) Luiti, G.; Dondes, S.; Harteck, P. *J. Chem. Phys.* **1966**, *44*, 4051.
(23) Chen, M. C.; Taylor, H. A. *J. Chem. Phys.* **1957**, *27*, 857.
(24) Laffon, C.; Lacombe, S.; Bournel, F.; Parent, Ph. *J. Chem. Phys.* **2006**, *125*, 204714.
(25) Johnson, R. E.; Quickenden, T. I. *J. Geophys. Res.* **1997**, *102*, 10985.
(26) Schuchmann, H.-P.; Wagner, R.; Von Sonntag, C. *Int. J. Radiat. Biol.* **1986**, *50*, 1051.
(27) Seiki, H.; Nagai, R.; Imamura, M. *Bull. Chem. Soc. Jpn.* **1968**, *41*, 2877.
(28) Baulch, D. L.; Bowman, C. T.; Cobos, C. J.; Cox, R. A.; Just, Th.; Kerr, J. A.; Pilling, M. J.; Stocker, D.; Troe, J.; Tsang, W.; Walker, R. W.; Warnatz, J. *J. Phys. Chem. Ref. Data* **2005**, *34*, 757.
(29) Stief, H. J.; Nava, D. F.; Payne, W. A.; Michael, J. V. *J. Chem. Phys.* **1980**, *75*, 2254.
(30) Hynes, A. J.; Wine, P. H.; Ravishankara, A. R. *J. Geophys. Res.* **1986**, *91* (D11), 815.
(31) Watanabe, N.; Kouchi, A. *Astrophys. J.* **2002**, *567*, 651.

JP904534A